Resonant structures in the $^{16}O(^{16}O,^{12}C)^{20}Ne$ reaction

Yosio Kondō* and Taro Tamura
Department of Physics, University of Texas, Austin, Texas 78712
(Received 17 October 1983)

Formulation is made of an exact finite-range distorted-wave Born approximation for the case in which the distorting potentials depend on the total angular momentum J. The general formula thus derived is then simplified for the cases in which the spins of the projectile, target, and ejectile are zero. This simplified form of the new exact finite-range distorted-wave Born approximation formula is applied to the analyses of the resonant structures seen in the $^{16}O(^{16}O,^{12}C)^{20}Ne(4_1^+)$ reaction, and it is found that good fits to data are obtained. It is also shown that the mechanism embodied in the band crossing model plays an essential role in achieving these good fits. A detailed discussion concerning the absolute magnitude of the distorted-wave Born approximation cross sections is also presented, based on recent calculations which use the cluster model.

I. INTRODUCTION

Recently the present authors proposed that the study of resonant phenomena in heavy-ion induced transfer reactions be carried out within the distorted-wave Born approximation (DWBA) framework with an interpretation based upon the band crossing model.[1] The first successful demonstration of this approach involved analyses[2] of the resonant structures seen in the $^{16}O(^{16}O,^{12}C)^{20}Ne$ reaction. Subsequently, similarly successful analyses were reported for a variety of heavy-ion induced transfer reactions: $^{14}C(^{12}C,^{13}C(\frac{5}{2}^+))^{13}C$ (Ref. 3), $^{14}C(^{16}O,^{18}O(2^+))^{12}C$ (Ref. 3), $^{20}Ne(^{16}O,^{12}C)^{24}Mg$ (Ref. 4), and $^{24}Mg(^{16}O,^{12}C)^{28}Si$ (Ref. 5).

An important feature common to most of these calculations[2,4,5] is the use of so-called J-dependent optical potentials[6] in the DWBA calculations. Surface transparent potentials of the Gobbi type[7] have often been thought to simulate the effects of J-dependent optical potentials, at least, for elastic scattering. However, in Ref. 2, we showed that these two kinds of potentials predicted markedly different excitation functions for the $^{16}O(^{16}O,^{12}C)^{20}Ne(4_1^+)$ reaction, and that the J-dependent potential resulted in a better reproduction of the observed gross structures. More recently, Robson and Smith[5] also demonstrated that they were able to describe successfully the pronounced structures in the excitation functions for the $^{24}Mg(^{16}O,^{12}C)^{28}Si(g.s.)$ reaction, when they used a J-dependent potential, but were unable to do so if a Gobbi-type potential was used.

In the present paper, we shall discuss first a general formulation of the DWBA calculations in which the distorting potentials have an explicit total angular momentum (J) dependence. The obtained formula is certainly more complicated than that used in the usual DWBA, where potentials are J independent. However, for certain types of transfer reactions, in which the spins of the projectile, target, and ejectile are zero, this DWBA formula can be very much simplified. The simplified formula will also be given.

The $^{16}O(^{16}O,^{12}C)^{20}Ne$ reaction was the first heavy-ion transfer reaction in which the presence of prominent gross structures was observed.[8,9] As we remarked above, we have previously studied this reaction, and some of those results have been reported in short papers.[2] In the present paper, we intend to present the results of our exact finite range (EFR) DWBA analyses of the $^{16}O(^{16}O,^{12}C)^{20}Ne(4_1^+)$ reaction in detail. It will be seen that the available experimental data[8,9] are reproduced rather well this way. It will also be shown that, in achieving these good fits, the enhancement mechanism embodied in the band crossing model[1] is playing a key role.

For the $^{16}O(^{16}O,^{12}C)^{20}Ne$ reaction, Arima *et al.*[10] studied, at a fixed energy [$E_{lab}(^{16}O)=60$ MeV], the problem of calculating the absolute DWBA cross section. This was done ten years ago, and they did this by using the no-recoil and Buttle-Goldfarb[11] approximations. Since we are now capable of performing much improved calculations, we decided to take up this problem again, and the results of this investigation will also be discussed in the present paper.

The DWBA formulae are presented in Sec. II, and the results of the analyses are presented in Sec. III. In Sec. IV we discuss the absolute cross section problem. A summary and conclusions of the present work are given in Sec. V.

II. FORMALISM

In this section we present a DWBA formalism in which the distorting potentials depend explicitly on the total angular momentum J of the system. Because of this J dependence, the distorted waves also become J dependent, and the DWBA formula becomes more complicated than that with the conventional J-independent potentials.[12,13] In the following, we use the notation of Ref. 13.

Equations (1)—(3) give the general DWBA formula for a transfer reaction $A(a,b)B$ in which the distorted waves, $\chi^J_{l_a}$ and $\chi^J_{l_b}$, have an explicit J dependence:

$$\frac{d\sigma^{J\,\mathrm{dep}}}{d\Omega}(\theta)=\frac{\mu_a\mu_b}{(2\pi\hbar^2)^2}\frac{k_b}{k_a}\frac{1}{(2I_A+1)(2s_a+1)}\sum_{\substack{M_AM_B\\ m_am_b}}\left|T^{J\,\mathrm{dep}}_{M_Bm_b;M_Am_a}(\theta)\right|^2 , \tag{1}$$

$$T^{J\,\mathrm{dep}}_{M_Bm_b;M_Am_a}(\theta)=\frac{4\pi}{k_ak_b}\hat{s}_>\hat{I}_>(-)^{I_A-I_B}\sum_{jls}\sum_{\substack{l_bm_{l_b}\\ j_bm_{j_b}}}\sum_{\substack{l_aJM\\ j_am_{j_a}}}(-)^{j_a-s_b-l_b}\epsilon^{js}_{AaBb}(l_a0s_am_a\,|\,j_am_{j_a})(j_am_{j_a}I_AM_A\,|\,JM)$$

$$\times(l_bm_{l_b}s_b-m_b\,|\,j_bm_{j_b})(j_bm_{j_b}I_B-M_B\,|\,J-M)\hat{l}_a\hat{l}_b\hat{l}^2\hat{s}\hat{j}_a\hat{j}_b\hat{j}$$

$$\times I^{jls;AaBb}_{l_bJ;l_aJ}W(j_aj_bI_AI_B;jJ)\begin{Bmatrix}l_a & s_a & j_a\\ l_b & s_b & j_b\\ l & s & j\end{Bmatrix}G_{l_b-m_{l_b}}P_{l_b\,|\,m_{l_b}|}(\cos\theta) , \tag{2}$$

where the overlap integral $I^{jls;AaBb}_{l_bJ;l_aJ}$ is the analog of Eq. (2.19) of Ref. 13 and is given by

$$I^{jls;AaBb}_{l_bJ;l_aJ}=\frac{1}{2l+1}\sum_{m_l}\mathscr{T}\int\int d\vec{r}_a d\vec{r}_b\left\{\sum_{\substack{l_1n_1\\ l_2n_2}}d^{jls;AaBb}_{l_1n_1l_2n_2}f^{l_1n_1l_2n_2}_{\tilde{l}m_l}(\vec{r}_1,\vec{r}_2)\right\}(r_ar_b)^{-1}\{\chi^J_{l_b}(k_b,r_b)\chi^J_{l_a}(k_a,r_a)[Y_{l_a}(\hat{\vec{r}}_a)Y_{l_b}(\hat{\vec{r}}_b)]_{lm_l}\} . \tag{3}$$

The factors $s_>$, $I_>$, and ϵ^{js}_{AaBb} are defined in Eq. (2.15b) of Ref. 13 and were introduced to incorporate both pickup and stripping reactions into a single formula. G_{lm}, $d^{jls;AaBb}_{l_1n_1l_2n_2}$, and $f^{l_1n_1l_2n_2}_{\tilde{l}m_l}(\vec{r}_1,\vec{r}_2)$ are defined in Eqs. (2.20), (2.15a), and (2.13b), of Ref. 13, respectively, while $\mathscr{T}$ is the Jacobian needed in the coordiante transformation. As the technique for handling the sixfold integral in Eq. (3) has been discussed elsewhere,[12,13] we will not repeat it. It should be noted that the present formulation is quite general and the same formula can also be used for the case in which the distorting potentials include a spin-orbit interaction in addition to a J-dependent interaction. [In Refs. 13 and 14, a formulation was given for the case in which the distorting potentials include a spin-orbit interaction. This formula is slightly simpler than the present formula of Eqs. (1)—(3), since the former does not include the J dependence of the potentials.]

The conventional DWBA formula for heavy-ion reactions, which has been adopted in EFR-DWBA programs, such as LOLA (Ref. 15) and SATURN-MARS,[16] is that of Eq. (2.25) of Ref. 13, and is expressed as

$$\frac{d\sigma}{d\Omega}(\theta)=\frac{\mu_a\mu_b}{(2\pi\hbar^2)^2}\frac{k_b}{k_a}\frac{(2I_>+1)}{(2I_A+1)}\frac{(2s_>+1)}{(2s_a+1)}\left[\frac{4\pi}{k_ak_b}\right]^2$$

$$\times\sum_{jls}\sum_{m_{l_b}}\left|\sum_{l_al_b}\hat{l}_a\hat{l}_b(l_a0l_bm_{l_b}\,|\,lm_{l_b})I^{jls;AaBb}_{l_b;l_a}(-)^{l_b+m_{l_b}}G_{l_b-m_{l_b}}P_{l_b\,|\,m_{l_b}|}(\cos\theta)\right|^2 . \tag{4}$$

In Eq. (4) $I^{jls;AaBb}_{l_b;l_a}$ is the same as $I^{jls;AaBb}_{l_bJ;l_aJ}$ of Eq. (3) except that the J dependence of the distorted waves in the latter is suppressed.

Comparison of Eqs. (1) and (4) shows that the DWBA formalism gets sufficiently more complicated, when the distorting potentials depend on J, that the conventional EFR-DWBA codes[15,16] cannot be used unless drastic modifications are made. Fortunately, however, we often encounter, in the regime of heavy-ion reactions, cases in which the spins of the projectile, target, and ejectile are zero, i.e., $s_a=I_A=s_b=0$. Under this situation, Eqs. (1) and (2) are very much simplified, resulting in

$$\frac{d\sigma^{J\,\mathrm{dep}}}{d\Omega}(\theta)=\frac{\mu_a\mu_b}{(2\pi\hbar^2)^2}\frac{k_b}{k_a}\left[\frac{4\pi}{k_ak_b}\right]^2(2I_>+1)\sum_{M_B}\left|\sum_{l_al_b}(-)^{l_b+M_B}\hat{l}_a\hat{l}_b(l_a0l_bM_B\,|\,I_BM_B)I^{jls;AaBb}_{l_bJ;l_aJ}G_{l_b-M_B}P_{l_b\,|\,M_B|}(\cos\theta)\right|^2 , \tag{5}$$

with, $J=l_a$, $s=0$, and $j=l=I_B$.

Equation (5) is identical to Eq. (4) (in which we also set $s_a=I_A=s_b=0$), except that the overlap integral $I^{jls;AaBb}_{l_bJ;l_aJ}$ of Eq. (5) depends on $J(=l_a)$. Therefore, for this simple case of $s_a=I_A=s_b=0$, the conventional EFR-DWBA programs can be used with only minor modifications to their structure. Our analyses of the ^{16}O(^{16}O,^{12}C)^{20}Ne reaction were done by modifying the SATURN-MARS program.[16]

Note that a further modification of the program is required to take into account the symmetry of the ^{16}O+^{16}O entrance channel for the ^{16}O(^{16}O,^{12}C)^{20}Ne reaction. This

can be achieved by suppressing all odd-J amplitudes and multiplying the even-J amplitudes by a factor of 2. In this way, both the α-particle pickup $^{16}O(^{16}O,^{20}Ne)^{12}C$ reaction and the α-particle stripping $^{16}O(^{16}O,^{12}C)^{20}Ne$ reaction are included in a consistent manner.

In our EFR-DWBA calculations, the transfer of an α cluster from an ^{16}O to another ^{16}O was assumed. The radial wave functions in the α-^{12}C and α-^{16}O systems were calculated by the separation energy method, using a Woods-Saxon potential with radius $1.35A_{\text{core}}^{1/3}$ fm and diffuseness 0.65 fm, the depths being adjusted to obtain the experimental α-particle separation energies in ^{16}O and ^{20}Ne, in addition to the Coulomb potential. The Coulomb radius of the uniform charge distribution was also taken to be $135A_{\text{core}}^{1/3}$ fm. The number of nodes was fixed according to the rule that

$$\sum_{i=1}^{4}(2N_i+L_i)=2n_\alpha+l_\alpha;\ \ (\alpha=1,2)\ . \tag{6}$$

In Eq. (6), (N_i,L_i) are shell model quantum numbers of the individual nucleons, (n_1,l_1) and (n_2,l_2) describe their center of mass motion with respect to the core, and $0s$ internal motion is assumed for the α particle. The post form was used consistently, unless stated otherwise. The adopted α-particle spectroscopic factors, $S_\alpha=0.30$ for ^{16}O and $S_\alpha=0.23$ for ^{20}Ne, were those of the SU(3) model.[17]

III. EFR-DWBA ANALYSES OF THE $^{16}O(^{16}O,^{12}C)^{20}Ne(4_1^+)$ REACTION

Recent experiments have demonstrated that resonant structures are observed not only in heavy-ion elastic and inelastic scattering, as has been known for some time now, but also in a wide range of heavy-ion induced transfer reactions; examples are $^{14}C(^{12}C,^{13}C)^{13}C$ (Ref. 18), $^{14}C(^{14}C,^{15}C)^{13}C$ (Ref. 19), $^{14}C(^{16}O,^{18}O)^{12}C$ (Ref. 20), $^{16}O(^{16}O,^{12}C)^{20}Ne$ (Refs. 8 and 9), $^{20}Ne(^{16}O,^{12}C)^{24}Mg$ (Ref. 21), and $^{24}Mg(^{16}O,^{12}C)^{28}Si$ (Refs. 22 and 23). In particular, for the $^{16}O(^{16}O,^{12}C)^{20}Ne$ reaction leading to the 4^+ member ($E_x=4.25$ MeV) of the ground band of ^{20}Ne, it was shown that excitation functions at several angles had pronounced gross structures with peak to valley ratios of up to ten, and that these structures were strongly correlated in their energies.[8,9] In this section we shall present the results of our EFR-DWBA analyses of this reaction.

A. Distorting potentials

There are several optical potentials known for the $^{16}O+^{16}O$ system (see Table I). The Maher potential[24] is a weakly-absorptive type with a four parameter Woods-Saxon form. The Gobbi potential[7] is a surface transparent type (six parameter form), in that the radius and diffuseness parameters of the imaginary part are smaller than those of the real part. The Chatwin[6] and Kondō, Bromley, and Abe (KBA) (Ref. 25) potentials are J dependent, and an increased transparency of the surface partial waves is introduced through a smooth cutoff of the absorptive potential, as J approaches a critical angular-momentum J_{cr}. This cutoff results from the requirement that the total angular momentum and energy must be simultaneously conserved in the open reaction channels. All the four optical potentials listed in Table I are known to successfully reproduce the gross energy dependence of the $^{16}O+^{16}O$ elastic scattering data.[24] It should be noted

TABLE I. Distorting potentials for the $^{16}O+^{16}O$ channel.

(1) Maher potential (Ref. 24)

$$U(r)=\frac{-17-i(0.4+0.1E_{\text{c.m.}})}{\{1+\exp[(r-6.8)/0.49]\}},\quad R_{\text{Coul}}=6.8\text{ fm}.$$

(2) Gobbi potential (Ref. 7)

$$U(r)=\frac{-17.0}{\{1+\exp[(r-R_0)/0.49]\}}-i\frac{0.8+0.2E_{\text{c.m.}}}{\{1+\exp[(r-R_i)/0.15]\}},$$

$$R_0=R_{\text{Coul}}=1.35(16^{1/3}+16^{1/3}),\quad R_i=1.27(16^{1/3}+16^{1/3}).$$

(3) Chatwin potential (Ref. 6)

$$U(r)=\left[-17.0-i\frac{0.22E_{\text{c.m.}}}{\{1+\exp[(J-J_{\text{cr}})/0.4]\}}\right]\frac{1}{\{1+\exp[(r-6.8)/0.49]\}},$$

$$J_{\text{cr}}=6.7[2\mu(E_{\text{c.m.}}-6.7)/\hbar^2]^{1/2},\quad R_{\text{Coul}}=6.8\text{ fm}.$$

(4) KBA potential (Ref. 25)

$$U(r)=\frac{100}{\{1+\exp[(r-3.5)/0.3]\}}+\left[-16.0-0.014L(L+1)-i\frac{0.3E_{\text{c.m.}}}{\{1+\exp[(J-J_{\text{cr}})/0.4]\}}\right]\frac{1}{\{1+\exp[(r-6.55)/0.5]\}},$$

$$J_{\text{cr}}=6.7[2\mu(E_{\text{c.m.}}-7.7)/\hbar^2]^{1/2},\quad R_{\text{Coul}}=6.55\text{ fm}.$$

TABLE II. Distorting potentials for the $^{12}C+^{20}Ne(4_1^+)$ channel. $E_{c.m.}$ refers to the center of mass energy of the $^{16}O+^{16}O$ channel.

(1) Vandenbosch potential (Ref. 26)

$$U(r)=\frac{-17-i(-0.333+0.54E_{c.m.})}{\{1+\exp[(r-R)/0.57]\}},\quad R=R_{Coul}=1.35(12^{1/3}+20^{1/3}).$$

(2) Gobbi potential (Ref. 7)

$$U(r)=\frac{-17.0}{\{1+\exp[(r-R_0)/0.49]\}},\quad -i\frac{0.314+0.2E_{c.m.}}{\{1+\exp[(r-R_i)/0.15]\}},$$

$$R_0=R_{Coul}=1.35(12^{1/3}+20^{1/3}),\quad R_i=1.27(12^{1/3}+20^{1/3}).$$

that the KBA potential which was originally introduced to use for coupled-channel calculations is also a good potential to use for uncoupled calculations, at least for the $^{16}O+^{16}O$ system, as was mentioned in Ref. 25. The knowledge of these optical potentials certainly facilitates our analyses, but it is also interesting to see whether these potentials behave differently, when they are used for transfer reactions involving resonances.

Unlike the entrance $^{16}O+^{16}O$ channel case, the knowledge of the optical model parameters to be used for the exit $^{12}C+^{20}Ne(4_1^+)$ channel is very limited. In the present analyses, we consider two potentials (see Table II): the strongly-absorptive Vandenbosch potential[26] and the weakly-absorptive Gobbi potential.[7] We shall discuss the implications of these potentials after presenting results obtained with their use.

B. Angular distribution

In Fig. 1, we first show a few theoretical angular distributions obtained for the $^{16}O(^{16}O,^{12}C)^{20}Ne(4_1^+)$ reaction at

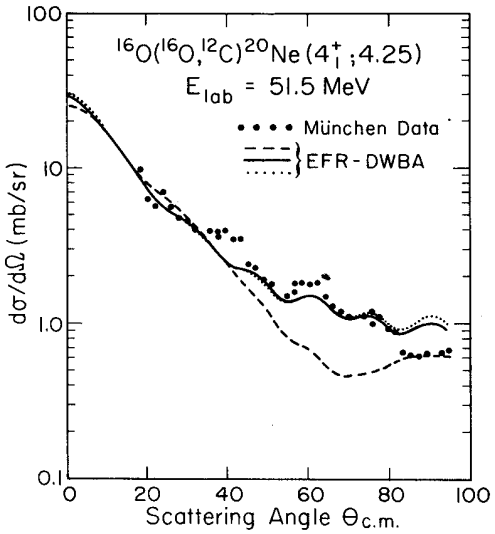

FIG. 1. Angular distributions of the $^{16}O(^{16}O,^{12}C)^{20}Ne(4_1^+)$ reaction at $E_{lab}(^{16}O)=51.5$ MeV. Data are those of Ref. 9. The dashed and solid lines, respectively, represent the EFR-DWBA cross sections with the KBA-Vandenbosch and KBA-Gobbi potentials. The post form was used for both calculations. The DWBA cross section with the prior form and the KBA-Gobbi potential is shown by the dotted line.

$E_{lab}(^{16}O)=51.5$ MeV, and compare them with the data of Rossner *et al.*[9] In this figure, the dashed line shows the DWBA cross section obtained by using the KBA-Vandenbosch potential, i.e., by using the KBA and Vandenbosch potentials for the entrance and exit channels, respectively. The predicted angular distribution has a slope which is too steep for $\theta_{c.m.}\gtrsim 40°$. The solid line shows the result with the KBA-Gobbi potential, i.e., with the KBA and Gobbi potentials for the incident and exit channels, respectively. In this case the experimental angular distribution is reproduced reasonably well. Certainly the weakly-absorptive Gobbi potential is preferred for the exit channel, rather than the strongly-absorptive Vandenbosch potential. The same preference was found when the other $^{16}O+^{16}O$ potentials of Table I were used for the entrance channel. The result with the prior form and with the KBA-Gobbi potential is also given in Fig. 1 by the dotted line, which demonstrates the practical equivalence of the post and prior forms. The DWBA cross sections shown in Fig. 1 were normalized to the data at forward angles. The normalization factor was 17 and 3.5 for the KBA-Vandenbosch and KBA-Gobbi cases, respectively. Essentially the same values of the normalization factor were used for all the DWBA cross sections reported in this section.

C. Excitation functions

The relative merits of the entrance channel optical potentials of Table I were not very clearly established by the predictions of the angular distribution at $E_{lab}(^{16}O)=51.5$ MeV discussed above, but became better established when the excitation functions were considered. The upper and lower panels of Fig. 2 show the excitation functions for the reaction at $\theta_{c.m.}=57°$ and 78°, respectively, and the data are again those of Ref. 9. In obtaining the theoretical results presented in this figure, the optical potential used for the exit channel was fixed to that of Gobbi which produced the better result in Fig. 1. The dotted lines in Fig. 2 show the DWBA excitation functions with the Gobbi-Gobbi potential. Although some structure was predicted, it was too weak compared with the data. The Maher-Gobbi potential, for which results are not shown in Fig. 2, had a similar difficulty. The dashed lines in Fig. 2 show the excitation functions with the Chatwin-Gobbi potential, and it is seen that the experimental resonant structures were reproduced reasonably well. It should be re-

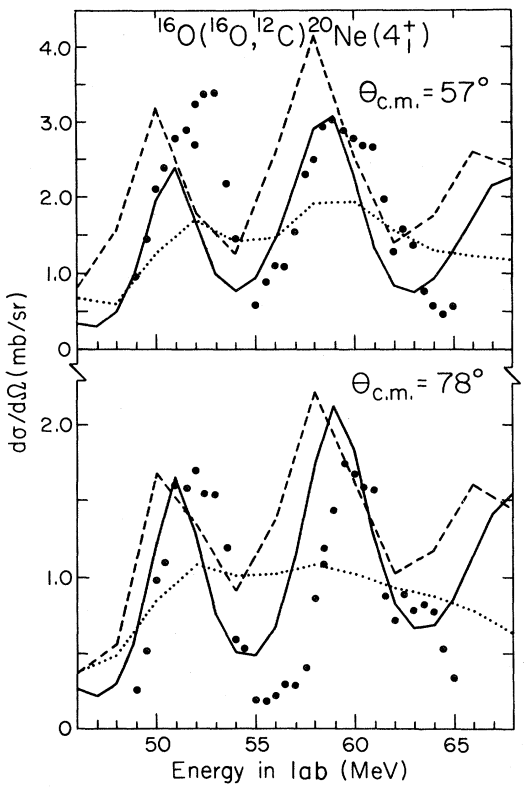

FIG. 2. Excitation functions of the $^{16}O(^{16}O,^{12}C)^{20}Ne(4_1^+)$ reaction at $\theta_{c.m.}=57°$ and 78°. Data are those of Ref. 9. The dotted, dashed, and solid lines represent the EFR-DWBA cross sections with the Gobbi-Gobbi, Chatwin-Gobbi, and KBA-Gobbi potentials, respectively. [The experimental cross sections given for the excitation functions (Ref. 9) appear to be too large by about a factor of 1.5, as seen by comparing the cross sections in the excitation functions, at $E_{lab}(^{16}O)=51.5$ MeV, with those given for the angular distribution (Ref. 9) at the same energy (see Fig. 1). The theoretical values were thus multiplied by a factor of 1.5 in this figure.]

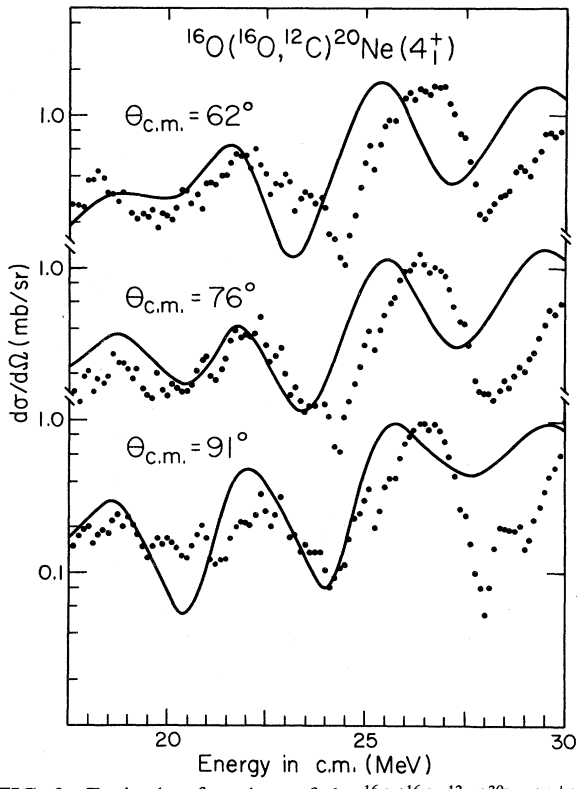

FIG. 3. Excitation functions of the $^{16}O(^{16}O,^{12}C)^{20}Ne(4_1^+)$ reaction at $\theta_{c.m.}=62°$, 76°, and 91°. Data are those of Ref. 8. The solid line represents the EFR-DWBA cross sections with the KBA-Gobbi potential.

called that the Chatwin potential has a J-dependent imaginary part. Since the Gobbi and the Chatwin potentials both have the same real part and predict quite similar excitation functions for $^{16}O+^{16}O$ elastic scattering, it is often conjectured that the effects of the "surface transparency" in the Gobbi potentials and the "J dependence of the imaginary part" in the Chatwin potential are basically equivalent. However, as seen in Fig. 2, they predict markedly different excitation functions for the transfer reaction.

The solid lines in Fig. 2 show the results obtained with the KBA-Gobbi potential. They are similar to those obtained with the Chatwin-Gobbi potential, but agree somewhat better with experiment. In fact, the energy interval, widths, and amplitudes of the gross structures are reproduced rather well, although the peak positions are still somewhat shifted to the lower energy side.

In Fig. 3, the results obtained with the KBA-Gobbi potential, which produced the best fit in Fig. 2, are compared with the data of Singh *et al.*[8] at $\theta_{c.m.}=62°$, 76°, and 91°. The energy region of the data is lower than that of Ref. 9 with reasonable overlap between the two measurements [remember that $E_{c.m.}=0.5\,E_{lab}(^{16}O)$ for the reaction]. A careful comparison between the two sets of data reveals the following: (i) there are noticeable systematic shifts in the energies of the resonant structures between the two experiments, and (ii) there is a disagreement in the absolute normalizations of the two experiments. The former is the reason why the shift of the theoretical peak positions relative to the data is more pronounced in Fig. 3 than it was in Fig. 2. The latter is the reason why the theoretical cross sections in Fig. 2 had to be multiplied by an overall factor of 1.5. In spite of these yet-unsettled experimental problems, we may conclude from the data of Ref. 8 that the gross resonant structures do persist into the lower $E_{c.m.}$ region with diminishing peak to valley ratios. Our results, presented in Fig. 3, reproduce this feature very well.

Excitation functions were also calculated with the KBA-Vandenbosch, the Chatwin-Vandenbosch, and the Gobbi-Vandenbosch potentials. In these cases, the predicted resonant structures were too weak.

D. Angle integrated cross section

A study of the angle integrated cross section has the advantage that this quantity is free from any angular effects

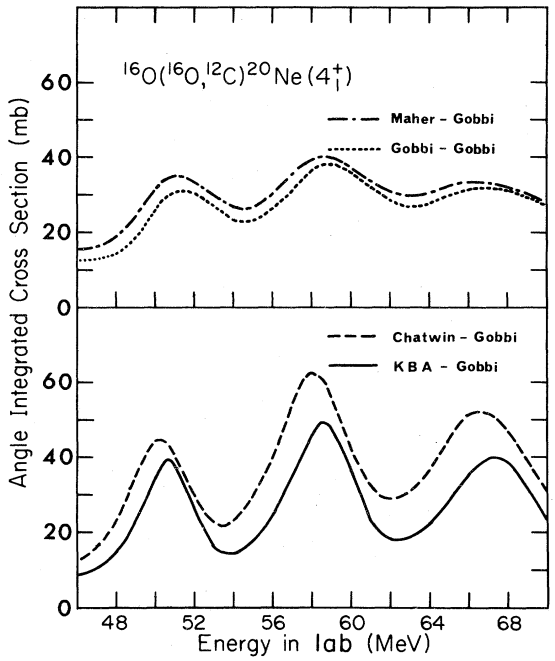

FIG. 4. Angle integrated cross sections of the $^{16}O(^{16}O,^{12}C)^{20}Ne(4_1^+)$ reaction. The four lines show the results of the EFR-DWBA calculations with potentials identified in the figure.

and so is likely to give a better criterion for the existence of resonances. In Fig. 4, we show angle integrated cross sections calculated with the four sets of potential pairs we used in the preceding subsection. It is seen that all four theoretical curves exhibit regular gross structures. It should be noted that even the case with the Gobbi-Gobbi potential (dotted line), for which not much structure was seen in Fig. 2, now shows more developed structures. The result with the Maher-Gobbi potential (dashed-dotted line) is similar. The structures with the Chatwin-Gobbi and KBA-Gobbi potentials (in the lower panel), are still better developed, being reminiscent of the structures of the excitation function data[8,9] seen in Figs. 2 and 3. Recently, Kolata *et al.*[27] measured, by using γ-ray techniques, the angle integrated ^{20}Ne yield produced from the $^{16}O + {}^{16}O$ incident channel. Their data show pronounced regular structures, which are correlated with the structures in the $^{16}O + {}^{16}O(3_1^-)$ inelastic scattering. The excitation functions we obtained in the lower panel of Fig. 4 are in line with Kolata's data.

It may be worth noting from Fig. 4 that the peak positions predicted with the Chatwin-Gobbi potential appear at the lower energy side, compared with those predicted with the Gobbi-Gobbi potential. This is in spite of the fact that the Gobbi and Chatwin potentials have the same real part, and can be explained as follows. In the Chatwin potential, the critical angular momentum J_{cr} depends on $E_{c.m.}$ (see Table I), and tends to reduce the resonant cross section at the higher energy side, thus shifting the position of the peaks to the lower energy side. A similar trend exists for the case using the KBA potential.

E. Mechanism of enhancement

Absolute squares of the DWBA overlap integrals $I_{L_f:L_i}$, which are to be identified with $I_{l_bJ;l_aJ}^{jls;AaBb}$ of Eq. (3) with $l_a=J=L_i$ and $l_b=L_f$, are shown in Fig. 5 for the KBA-Gobbi case which gave the best fits to the available $^{16}O(^{16}O,^{12}C)^{20}Ne(4_1^+)$ data. As seen, only one or two grazing partial waves are contributing strongly at any chosen energy. It is also seen that the resonances are dominated by the aligned configuration,[1] in which the orbital angular momentum L and the channel spin I are coupled to give the maximum total angular momentum J, i.e., in which $J=L+I$. In this case, the entrance channel orbital angular momentum L_i equals J, while the exit channel orbital angular momentum L_f equals $J-4$ $(=L_i-4)$.

As seen from the solid lines in Fig. 5, the overlap integrals of the aligned configuration are indeed very large at every peak energy of the calculated excitation functions (see Fig. 2). At $E_{lab}(^{16}O)=51$ and 59 MeV, the partial waves with $J=18$ and 20, respectively, make the dominant contributions. The strong enhancement of the overlap integral of the aligned configuration reflects the simultaneous onset of potential resonances in both the entrance and exit channels, and this is precisely the mechanism embodied in the band crossing model[1] for giving the enhanced structure.

That this is in fact the case is further seen in the schematic band crossing diagram in Fig. 6, in which the

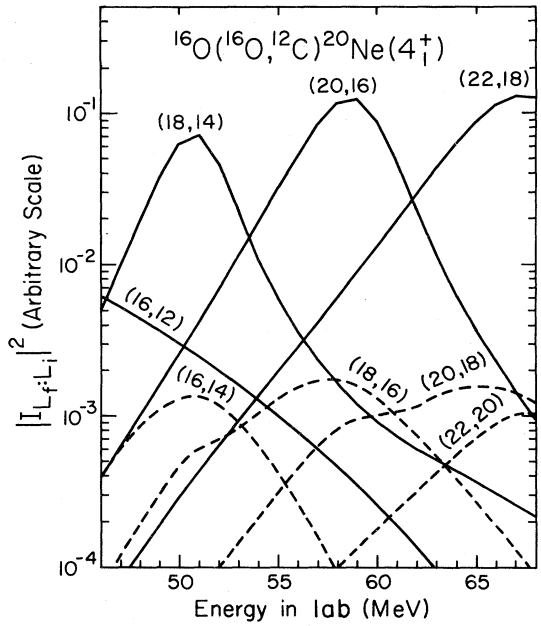

FIG. 5. Absolute square of the DWBA overlap integrals, $|I_{L_f:L_i}|^2$, of the $^{16}O(^{16}O,^{12}C)^{20}Ne(4_1^+)$ reaction for the case with the KBA-Gobbi potential. Associated with each curve is the pair of orbital angular momenta, (L_i,L_f). The solid lines show contributions from the aligned configuration, in which $L_f=L_i-4$. The dashed lines are those with $L_f=L_i-2$ configuration.

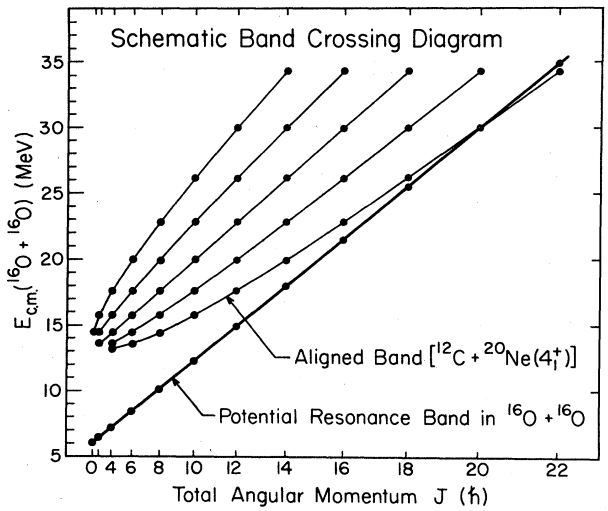

FIG. 6. Schematic diagram showing the crossing of the aligned band of the $^{12}C+^{20}Ne(4_1^+)$ channel with that of the incident $^{16}O+^{16}O$ channel. For further details of the band crossing model, see Ref. 1.

aligned band in the $^{12}C+^{20}Ne(4_1^+)$ channel crosses with the potential resonance band in the $^{16}O+^{16}O$ channel. This is a kind of double-resonance mechanism.[28] It should be noted that the band crossing model has also been applied successfully in explaining resonances in inelastic scattering in the $^{12}C+^{12}C$ (Ref. 29), $^{12}C+^{16}O$ (Ref. 30), and $^{16}O+^{16}O$ (Ref. 25) systems.

The $|I_{L_f:L_i}|^2$ values for the $L_f=L_i-2$ configuration, shown by dashed lines in Fig. 5, are much smaller compared with those for $L_f=L_i-4$ (solid lines). This is because, for $L_f=L_i-2$, the potential resonances in the two channels do not occur simultaneously (see also Fig. 6). It should be noted that, in this reaction, the kinematic matching condition[31] also favors the contribution of the aligned configuration. Contributions of the other configurations, i.e., $L_f=L_i$, L_i+2, and L_i+4, were found to be much smaller and are not shown in Fig. 5.

An Argand diagram of the DWBA overlap integral, $I_{14:18}$, obtained with the KBA-Gobbi potential is shown in Fig. 7. This diagram shows that $I_{14:18}$ reaches its maximum at about $E_{lab}(^{16}O)=51$ MeV and has a counterclockwise energy dependence. It is thus quite legitimate to conclude that the peaks of the excitation functions can be attributed to the onset of resonances.

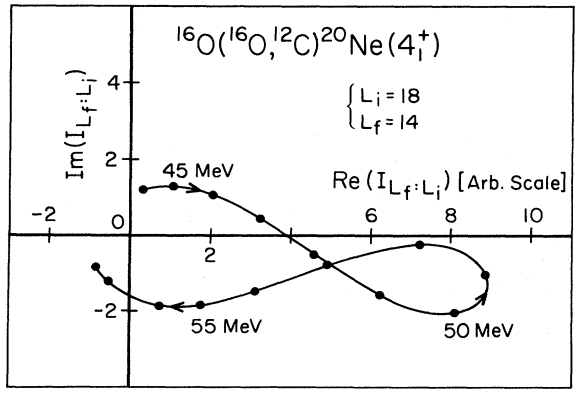

FIG. 7. Energy dependence of the DWBA overlap integral $I_{14:18}$ for the $^{16}O(^{16}O,^{12}C)^{20}Ne(4_1^+)$ reaction. Circles were placed at every 1 MeV interval of the incident energy $E_{lab}(^{16}O)$.

F. Discussion on distorting potentials in the $^{12}C+^{20}Ne(4_1^+)$ channel

We have used the Vandenbosch potential[26] in some of the calculations given above, and showed that we cannot use such a strongly-absorptive potential in the $^{12}C+^{20}Ne(4_1^+)$ channel. This potential was originally extracted by fitting the $^{12}C+^{20}Ne(0_{gr}^+)$ elastic scattering data,[26] which revealed much weaker oscillations (in both the angular distribution and excitation function) than those seen in $^{16}O+^{16}O$ elastic scattering.[24] Comparison of the present work and that of Vandenbosch *et al.*[26] shows that the imaginary potential in the $^{12}C+^{20}Ne(4_1^+)$ channel should be much weaker than that in the $^{12}C+^{20}Ne(0_{gr}^+)$ channel. That this is not unexpected can be seen as follows. Vandenbosch *et al.* showed that the $^{12}C+^{20}Ne(0_{gr}^+)$ channel can be more absorptive than is the $^{16}O+^{16}O$ channel, because the former couples strongly with a larger number of direct reaction channels than does the latter. A similar line of argument then allows us to expect that the $^{12}C+^{20}Ne(4_1^+)$ channel with the aligned configuration, which plays the dominant role in our transfer reaction, can be more weakly absorptive than is the $^{12}C+^{20}Ne(0_{gr}^+)$ channel. Thus, the present work and that of Ref. 26 are not in contradiction. It may, nevertheless, be worthwhile to note that there is some indication that the Vandenbosch potential is somewhat too absorptive to reproduce features of the $^{12}C+^{20}Ne$ fusion cross section.[32]

IV. ABSOLUTE VALUE OF THE DWBA CROSS SECTIONS

In Sec. III, we showed that the gross resonant structures of the $^{16}O(^{16}O,^{12}C)^{20}Ne(4_1^+)$ reaction were well reproduced, if we used the KBA-Gobbi potential. Based on this success, we shall now discuss the problem of predicting the absolute value of the cross sections.

This problem was considered by Arima *et al.*[10] about ten years ago, when EFR-DWBA calculations were not yet so commonly used. Instead they used the no-recoil (NR) and Buttle-Goldfard (BG) (Ref. 11) approximations. In view of our present knowledge of the EFR-DWBA method, the use of these approximations is hard to justify in heavy-ion induced transfer reactions. In any case, Arima *et al.* calculated the $^{16}O(^{16}O,^{12}C)^{20}Ne(4_1^+)$ cross section at $\theta_{c.m.}=15°$ with $E_{lab}(^{16}O)=60$ MeV, and obtained a very small value, $d\sigma/d\Omega=5.97\times10^{-3}$ mb/sr, when they used as the *transfer interaction* (i.e., as the DWBA interaction that causes the transfer reaction) the conventional form (i.e., the interaction that binds the α to ^{16}O to form ^{20}Ne; case II of Ref. 10). Arima *et al.* then showed that the DWBA cross section was increased by a factor of about 86, if the real part of the $\alpha+^{16}O$ optical potential was used for the transfer interaction (case IV of Ref. 10). Note also that the distorting potentials used were of a strongly-absorptive type.

In Sec. III, we have already made a statement about the absolute cross section (see the text pertaining to Fig. 1). In the present section, however, we wish to improve the calculation by using a form factor which is based on the cluster model, instead of using $R=1.35A_{\text{core}}^{1/3}$ fm and $a=0.65$ fm as done in Sec. III. For this purpose, we used the results of recent cluster model calculations, successfully performed for ^{16}O and ^{20}Ne in Refs. 33 and 34, respectively.

According to the microscopic point of view,[35] the bound state wave functions to be used in the DWBA calculation of the ^{16}O(^{16}O,^{12}C)^{20}Ne(4_1^+) reaction should be the reduced α-width amplitudes, denoted as $\mathscr{Y}_{^{16}\text{O}}(r)$ and $\mathscr{Y}_{^{20}\text{Ne}}(r)$, of the systems $\alpha+^{12}$C(^{16}O) and $\alpha+^{16}$O(^{20}Ne). For the ^{20}Ne system, this amplitude is given by

$$\mathscr{Y}_{^{20}\text{Ne}}(r)=\begin{bmatrix}20\\4\end{bmatrix}^{1/2} r\langle Y_{l0}(\Omega)\Phi_\alpha\Phi_{^{16}\text{O}}\,|\,\Phi_{^{20}\text{Ne}}\rangle\ , \tag{7}$$

where Φ_α, $\Phi_{^{16}\text{O}}$, and $\Phi_{^{20}\text{Ne}}$ represent the internal wave functions of α, ^{16}O, and ^{20}Ne, respectively. When the shell model SU(3)-(8,0) wave function is assumed for ^{20}Ne(4_1^+), we have

$$\mathscr{Y}^{\text{sm}}_{^{20}\text{Ne}}(r)=\sqrt{S_{\text{sm}}}\,u_{2,4}(r)\ , \tag{8}$$

where S_{sm} ($=0.23$) represents the SU(3) spectroscopic factor of ^{20}Ne, while $u_{2,4}(r)$ represents the normalized harmonic oscillator wave function with the nodal quantum number $n=2$ and the relative angular momentum $l=4$. Since $u_{n,l}(r)$ does not have the correct asymptotic behavior, Arima *et al.* simulated $u_{n,l}(r)$ by a normalized wave function $\psi_{\text{sm}}(r)$ obtained by the separation energy method which guarantees the correct asymptotic behavior. Then the product $\sqrt{S_{\text{sm}}}\psi_{\text{sm}}(r)$ was used for the reduced α-width amplitude. However, recent cluster model studies[36] have shown that ^{20}Ne has a pronounced α clustering, and that the SU(3) wave function does not provide as good a description of ^{20}Ne as may have been thought.

The DWBA form factor may be improved by using the reduced α-width amplitude, obtained from the cluster model. For this purpose, we introduce a new amplitude $\psi_{\text{cl}}(r)$ as

$$\psi_{\text{cl}}(r)=1/\sqrt{S_{\text{cl}}}\,\mathscr{Y}_{\text{cl}}(r)\ , \tag{9}$$

where S_{cl} and $\mathscr{Y}_{\text{cl}}(r)$ are the cluster model spectroscopic factor and the cluster model reduced α-width amplitude, respectively. Since $S_{\text{cl}}=\langle\mathscr{Y}_{\text{cl}}\,|\,\mathscr{Y}_{\text{cl}}\rangle$, $\psi_{\text{cl}}(r)$ is a normalized wave function. Then, $\psi_{\text{cl}}(r)$ may be simulated by a normalized wave function $\psi_{\text{ws}}(r)$ obtained by the separation energy method, and the product $\sqrt{S_{\text{cl}}}\psi_{\text{ws}}(r)$ thus obtained may finally be used as the reduced α-width amplitude. In the present calculation, the result of Bandō,[34] which took into account both the α clustering and the core polarization, was used for S_{cl} and $\mathscr{Y}_{\text{cl}}(r)$ in Eq. (9).

It was found that a good simulation of $\psi_{\text{cl}}(r)$ with Bandō's $\mathscr{Y}_{\text{cl}}(r)$ could be achieved in the separation energy method by using the parameters $R=1.25(16)^{1/3}$ fm and $a=0.80$ fm. Although a much more complicated method[35] using a nonlocal operator was proposed to simulate $\mathscr{Y}_{\text{cl}}(r)$, the use of the above method is sufficiently good for our purpose. Note that the use of the rather large value of the diffuseness parameter, $a=0.8$ fm, is important in simulating correctly the characteristic features of $\mathscr{Y}_{\text{cl}}(r)$, i.e., a small amplitude in the internal region and an enhanced tail in the external region.

For the $\alpha+^{12}$C system, the same procedure was performed to simulate the $\mathscr{Y}_{\text{cl}}(r)$ of Suzuki.[33] Because of the closed shell nature of ^{16}O(0_{gr}^+), the parameters obtained, $R=1.05(12)^{1/3}$ fm and $a=0.5$ fm, are almost the same as those of Ref. 10, which simulated the harmonic oscillator wave function $u_{2,0}(r)$ [see Eq. (8)]. The relation $S_{\text{cl}}=S_{\text{sm}}$ was assumed for this system.

The cross section at $\theta_{\text{c.m.}}=15°$ and $E_{\text{lab}}(^{16}\text{O})=60$ MeV, obtained by using the EFR-DWBA and the new form factor, was found to be 1.81 mb/sr, which is larger than the case II result of Ref. 10 by about a factor of 300. In order

TABLE III. DWBA cross sections for the ^{16}O(^{16}O,^{12}C)^{20}Ne(4_1^+) reaction at $E_{\text{lab}}(^{16}\text{O})=60$ MeV and $\theta_{\text{c.m.}}=15°$. For the explanation of each column see the text.

Ref. 10	Present	$d\sigma/d\Omega$ (mb/sr)	Increment factor
NR and BG	EFR-DWBA	0.042	7.0
Unsymmetrized	symmetrized	0.042	1.0
Prior form	post form	0.047	1.1
Strongly-absorptive potentials[a]	KBA-Gobbi potential[b]	0.252	5.4
Simulate harmonic oscillator wave functions for form factor[c]	simulate cluster model wave functions[d]	1.81	7.2

[a]For both the ^{16}O+^{16}O and ^{12}C+^{20}Ne channels, Woods-Saxon potential with the following parameters: $V=-100$ MeV, $R_r=1.19(A_1^{1/3}+A_2^{1/3})$ fm, $a_r=0.48$ fm, $W=-25$ MeV, $R_i=1.26(A_1^{1/3}+A_2^{1/3})$ fm, $a_i=0.26$ fm, and $R_c=1.45(A_1^{1/3}+A_2^{1/3})$ fm.

[b]For parameters, see Tables I and II.

[c]$\alpha+^{12}$C: $R=0.60(12^{1/3}+4^{1/3})$ fm, $a=0.5$ fm, $S_{\text{sm}}=0.30$, $\alpha+^{16}$O: $R=0.75(16^{1/3}+4^{1/3})$ fm, $a=0.5$ fm, $S_{\text{sm}}=0.23$.

[d]$\alpha+^{12}$C: $R=1.05\times12^{1/3}$ fm, $a=0.5$ fm, $S_{\text{cl}}=0.30$, $\alpha+^{16}$O: $R=1.25\times16^{1/3}$ fm, $a=0.8$ fm, $S_{\text{cl}}=0.24$.

to make it easy to see where this large difference came from, we prepared Table III. In the first column of this table, there are listed five items which characterize the calculation of Ref. 10, while in the second column we show how each of these five conditions was replaced by our improved calculation. As each of these items was replaced one by one, the calculated cross section increased accordingly, and the newly obtained cross sections are listed in the third column. Note that we started with 5.97×10^{-3} mb/sr of case II of Ref. 10, and the factors with which the cross section was increased in each step of the above replacement are listed in the fourth column. As seen, items 2 and 3 did not produce a large difference. On the other hand, the items 1, 4, and 5 contributed about equally in bringing about the above-mentioned difference of the factor 300.

We have also studied the case using the transfer interaction used in case IV of Ref. 10. With the other conditions the same as those of the second column of Table III, the use of this new interaction gave a cross section of 101 mb/sr (compare this with 0.508 mb/sr in Ref. 10). It should be noted that, when we used the prior form, the cross section became 31.3 mb/sr. Thus, with this choice of the transfer interaction, the post-prior equivalence is violated, a result which is not totally unexpected; it destroys the basic structure of the DWBA theory.

The above-mentioned cross sections are to be compared with the experimental measurement of the $^{16}O(^{16}O,^{12}C)^{20}Ne(4_1^+)$ cross section at $E_{lab}(^{16}O)=60$ MeV and $\theta_{c.m.}=15°$. Since no experimental information is available for it, however, we estimated it by extrapolating the results given in Sec. III, and found it would be about 13 mb/sr. According to this value, our result, 1.81 mb/sr, given above, is underestimating the "experiment" by a factor of 7. (On the other hand, the use of the new transfer interaction makes the theory overestimate the "experiment" by a factor of 8.)

Finally, it should be noted that we have repeated all the EFR-DWBA calculations of Sec. III by using again the KBA-Gobbi potential and now using the improved form factor. All the characteristics of the results presented in Sec. III were reproduced with these new calculations except that the normalization factor $N=3.5$, which we needed in Sec. III, has now been replaced by $N=7$.

V. SUMMARY AND CONCLUSIONS

In the present paper we have presented a general formulation of the DWBA calculations in which the distorting potentials have an explicit J dependence. This J-dependent DWBA formula is more complicated than that used in the usual DWBA, where potentials are J independent. It has been shown that for certain types of transfer reactions in which the spins of the projectile, target, and ejectile are zero, this formula can be very much simplified and that conventional J-independent EFR-DWBA codes can be used for numerical calculations of this simple case with only relatively minor changes to their structure.

Based on this simplified formula, extensive calculations were carried out to analyze the data of the $^{16}O(^{16}O,^{12}C)^{20}Ne(4_1^+)$ reaction, which revealed well-developed gross resonant structures.[8,9] We have shown that the angular distribution and excitation functions of the data are reproduced fairly well by the EFR-DWBA calculations. In obtaining these good fits, the KBA potential[25] and the Gobbi potential[7] were used in the entrance and exit channels, respectively.

The peaks of the calculated excitation functions were shown to be associated with enhancement of the DWBA overlap integral for the aligned configuration. This enhancement reflects the simultaneous onset of potential resonances in both the entrance and exit channels, as is predicted by the band crossing model.[1] It should be noted that this enhancement mechanism is common to all the successful DWBA analyses of the resonant structures in heavy-ion transfer reactions reported to data.[2–5]

As demonstrated and emphasized, it was vital to have weakly-absorptive potentials in both channels. It was further shown that the present analyses were even capable of discriminating between weakly-absorptive potentials, as exemplified by the comparison of the Gobbi-Gobbi and the Chatwin-Gobbi curves in Figs. 2 and 4. For the entrance $^{16}O+^{16}O$ channel, the J-dependent type optical potentials[6,25] provided better reproduction of the data than the Gobbi-type surface transparent potential.

We also have discussed in some detail the problem of the absolute magnitude of the EFR-DWBA cross sections. It was shown that the theoretical cross section at $E_{lab}(^{16}O)=60$ MeV and $\theta_{c.m.}=15°$ for the $^{16}O(^{16}O,^{12}C)^{20}Ne(4_1^+)$ reaction is increased, by careful choice of the various conditions of the DWBA calculation, by about a factor of 300 compared with that calculated by Arima *et al.*[10] Among the differences between these two calculations, the changes from the Buttle-Goldfarb approximation to the EFR-DWBA, from the shell model form factor to the cluster model form factor, and from the strongly-absorptive potentials to the weakly-absorptive KBA-Gobbi potential are the dominant sources of the drastic increase of the cross section obtained.

In spite of the drastic improvement, the DWBA cross section is still a factor of 7 smaller than the "experiment." This fact may indicate that DWBA calculations for composite particle transfer reactions need some modification. We also studied the effect of a modification of the transfer interaction as proposed by Arima *et al.*[10] When we incorporate the new transfer interaction into our EFR-DWBA calculation, the result overestimates the "experiment" by a factor of 8. Thus, while the present result cannot exclude the suggested transfer interaction, it indicates that the use of such a transfer interaction is not as attractive as was indicated in Ref. 10.

ACKNOWLEDGMENTS

We are grateful to Professor M. Ichimura for helpful discussions. We thank Dr. R. Smith and Dr. B. A. Robson for reading the manuscript and commenting on it. This work was supported in part by the U.S. Department of Energy.

*Present address: Department of Theoretical Physics, Research School of Physical Sciences, The Australian National University, Canberra, ACT 2601, Australia.

[1]Y. Abe, Y. Kondō, and T. Matsuse, Prog. Theor. Phys. Suppl. 68, 303 (1980), and references therein.

[2]Y. Kondō and T. Tamura, Phys. Lett. 109B, 171 (1982); in *Lecture Notes in Physics,* edited by K. A. Eberhard (Springer, Berlin, 1982), Vol. 156, p. 314.

[3]O. Tanimura, in *Lecture Notes in Physics,* edited by K. A. Eberhard (Springer, Berlin, 1982), Vol. 156, p. 372.

[4]Y. Kondō, B. A. Robson, and R. Smith, Nucl. Phys. A410, 289 (1983).

[5]B. A. Robson and R. Smith, Phys. Lett. 123B, 160 (1983).

[6]R. A. Chatwin, J. S. Eck, D. Robson, and A. Richter, Phys. Rev. C 1, 795 (1970).

[7]A. Gobbi, R. Wieland, L. Chua, D. Shapira, and D. A. Bromley, Phys. Rev. C 7, 30 (1973).

[8]P. P. Singh, D. A. Sink, P. Schwant, R. E. Malmin, and R. H. Siemssen, Phys. Rev. Lett. 28, 1714 (1972).

[9]H. H. Rossner, G. Hinderer, A. Weidinger, and K. A. Eberhard, Nucl. Phys. A218, 606 (1974).

[10]A. Arima, R. A. Broglia, M. Ichimura, and K. Schäfer, Nucl. Phys. A215, 109 (1973).

[11]P. J. A. Buttle and L. J. B. Goldfarb, Nucl. Phys. 78, 409 (1966).

[12]N. Austern, R. M. Drisko, E. C. Halbert, and G. R. Satchler, Phys. Rev. 133, B3 (1964).

[13]T. Tamura, Phys. Rep. 14, 59 (1974).

[14]G. R. Satchler, Nucl. Phys. 55, 1 (1964).

[15]R. M. DeVries (unpublished).

[16]T. Tamura and K. S. Low, Comput. Phys. Commun. 8, 349 (1974).

[17]M. Ichimura, A. Arima, E. C. Halbert, and T. Terasawa, Nucl. Phys. A204, 225 (1973).

[18]R. M. Freeman, F. Haas, and G. Korschinek, Phys. Lett. 90B, 229 (1980).

[19]R. M. Freeman, C. Beck, F. Haas, B. Heusch, H. Bohn, U. Kaüfl, K. A. Eberhard, H. Puchta, T. Senftleben, and W. Trautmann, Phys. Rev. C 24, 2390 (1981).

[20]J. J. Kolata, C. Beck, R. M. Freeman, F. Haas, and B. Heusch, Phys. Rev. C 23, 1056 (1981).

[21]J. Schimizu, W. Yokota, T. Nakagawa, Y. Fukuchi, H. Yamaguchi, M. Sato, S. Hanashima, Y. Nagashima, K. Furuno, K. Katori, and S. Kubono, Phys. Lett. 112B, 323 (1982).

[22]M. Paul, S. J. Sanders, J. Cseh, D. F. Geesaman, W. Henning, D. G. Kovar, C. Olmer, and J. P. Schiffer, Phys. Rev. Lett. 40, 1310 (1978).

[23]J. Nurzynski, T. R. Ophel, P. D. Clark, J. S. Eck, D. F. Hebbard, D. C. Weisser, B. A. Robson, and R. Smith, Nucl. Phys. A363, 253 (1981).

[24]J. V. Maher, M. W. Sachs, R. H. Siemssen, A. Weidinger, and D. A. Bromley, Phys. Rev. 188, 1665 (1969).

[25]Y. Kondō, D. A. Bromley, and Y. Abe, Phys. Rev. C 22, 1068 (1980).

[26]R. Vandenbosch, M. P. Webb, and M. S. Zisman, Phys. Rev. Lett. 33, 842 (1974).

[27]J. J. Kolata, R. M. Freeman, F. Haas, B. Heusch, and A. Gallmann, Phys. Rev. C 19, 2237 (1979).

[28]W. Scheid, W. Greiner, and R. Lemmer, Phys. Rev. Lett. 25, 176 (1970).

[29]Y. Kondō, Y. Abe, and T. Matsuse, Phys. Rev. C 19, 1356 (1979).

[30]T. Matsuse, Y. Abe, and Y. Kondō, Prog. Theor. Phys. 59, 1904 (1978).

[31]D. M. Brink, Phys. Lett. 40B, 37 (1972).

[32]P. A. DeYoung, J. J. Kolata, R. C. Luhn, R. E. Malmin, and S. N. Tripathi, Phys. Rev. C 25, 1420 (1982).

[33]Y. Suzuki, Prog. Theor. Phys. 56, 111 (1976).

[34]H. Bandō, Nucl. Phys. A261, 269 (1976).

[35]A. Arima, *Heavy Ion Collisions,* edited by R. Bock (North-Holland, Amsterdam, 1979), Vol. 1, p. 417.

[36]Y. Fujiwara, H. Horiuchi, K. Ikeda, M. Kamimura, K. Katō, Y. Suzuki, and E. Uegaki, Prog. Theor. Phys. Suppl. 68, 29 (1980), and references therein.